ROMANIAN JOURNAL OF INFORMATION SCIENCE AND TECHNOLOGY
Volume **14**, Number 4, 2011, 324–333

Longitudinal Elastic Waves in Deformed Carbon Nanotubes

Gergely KOSA, Mircea BERCU, Voicu GRECU

Faculty of Physics, University of Bucharest,
Măgurele-Bucureşti, Romania

E-mail: mircea_bercu2@yahoo.com

Abstract. This study investigates the exciting of the elastic waves in single walled carbon nanotubes (SWCNT) during their deformations according to the conditions of mechanical treatments. The assumed procedures for longitudinal deformation are related to a short time extension at different velocities and to a harmonic oscillation impose to the atoms placed at one end of the nanotube. We analyse the responses of SWCNT to the external mechanical actions by using a large atomistic model of 2200 atoms simulating a carbon nanotubes of 27.3 nm in the conditions of rigid couplings at its both ends using modified Morse inter-atomic potentials. The simulation models provides details about reversible and irreversible disruption of SWCNT manifested by local transitions to carbon nanowire and self healing processes, being related to the conditions of the mechanical treatments.

Keywords: Single-wall carbon nanotubes, elastic wave propagation, molecular dynamics.

1. Introduction

We investigate through molecular dynamics simulations the behavior of bridged single-walled carbon nanotubes, where a deformation is being applied at one extremity, the other one being fixed. At a high stretch rate, the carbon nanotube behaves as a non-homogeneous medium, due to non-uniform distribution of the strain along its length. The reflections and the interferences of the generated longitudinal elastic waves, which may influence tube fracturing processes, show a complex picture of

the studied atomic system, even from a classical mechanics point of view. Atomistic scale simulation is the most appropriate approach for a dynamic description of the stretched carbon nanotubes. These types of studies are of interest for potential nano-technologies on reassembling ordered SWCNT networks by tube fracturing and re-bonding processes under specific mechanic treatments.

As CNTs are extremely small, the experiments to measure the properties of individual nanotubes are quite difficult. Therefore, the computational simulations have been regarded as a powerful tool for studying the behavior of nano-structures at atomistic level, including investigating CNT properties [1]. In recent years, numerical modeling of carbon nanotube properties has gained significant attention in computational nano-science and its associated fields of computational condensed matter physics and materials modeling regarding mechanical, thermal and transport properties [2]. The energies and dynamics of the atoms are calculated using prescribed inter-atomic potentials, and the simulation involves the computation of forces experienced by each atom at each time step of the simulation from these potentials [3]. Inter-atomic potentials given by Tersoff [4] and Brenner [5] are common empirical potentials employed to investigate the mechanical properties of carbon nanostructures, and the Brenner potential function is generally considered more accurate and it is more versatile than the Morse potential, because it can handle bond hybridization and bonds with different atoms. However, as shown by Belytschko *et al.* [6], the Brenner potential it is affected by the cut-off function on treating the axial deformation and fracturing of SWCNT, therefore it is advisable in this particular case to work with the modified Morse potential already reported for these types of applications.

2. Method and atomistic model

For our molecular dynamics simulation, we consider an armchair (5, 5) single walled carbon nanotube, consisting of 2220 atoms, having a length of 273 Å and a diameter of 6.8 Å. The tube is in bridge configuration, *i.e.* both ends are attached to large masses, and may be initially relaxed or strained. We apply a deformation at the right end of the tube, and investigate the propagation of the longitudinal waves depending on the initial strain and the nature of deformation applied.

Expressions (1) and (2) represent the stretching and bending energy in a modified Morse potential of inter-atomic interactions:

$$E_{stretch} = E_0 \left[\left(1 - e^{-\beta(r-r_0)} \right)^2 - 1 \right], \tag{1}$$

$$E_{bend} = k_\theta \left(\theta - \theta_0 \right)^2 \left[1 + k_{sextic} \left(\theta - \theta_0 \right)^4 \right] / 2. \tag{2}$$

The above approximation neglects the weak contribution of dihedral angles to the total energy. We found that the parameters reported by Belytschko [5] lead to acceptable results, using the following values: $r_0 = 1.39$ Å, $E_0 = 3.75$ eV and $\beta = 2.625$ Å^{-1}, $\theta_0 = 120°$, $k_\theta = 5.625$ eV, $k_{sextic} = 0.754$ rad^{-4}.

We simulate three types of experiments. The first is associated to a fast elongation of the SWCNT at one end for a short time, usually for 3 picoseconds, after which the end becomes fixed again and the nanotube will stay in its new, strained position. In the second type of simulation, the strained end of the nanotube is moving in a forced oscillation at a given frequency. The third deformation type investigated in this study is continuous stretching of SWCNT until its failure.

The model could be related to the design of potential experiments involving a single or many bridged SWCNT anchored to a fixed wall at one end and to a retractile piezo-substrate at the opposite one.

3. Young modulus of SWCNT

The stress-strain dependency of (5, 5) SWCNT is presented in Fig. 1. This is very similar to experimental data reported for single-walled carbon nanotubes from scientific literature [7]. When the SWCNT is loaded above the yield strength, the cross section area decreases do to the plastic flow. It happened at the end of the saturated portion of the curve where the transition to zero of the stress indicates the tube failure. Young's modulus is calculated from the slope of this curve. Therefore the tangent modulus E_t can be defined for various strain levels by computing the corresponding tangent of the stress-strain curve.

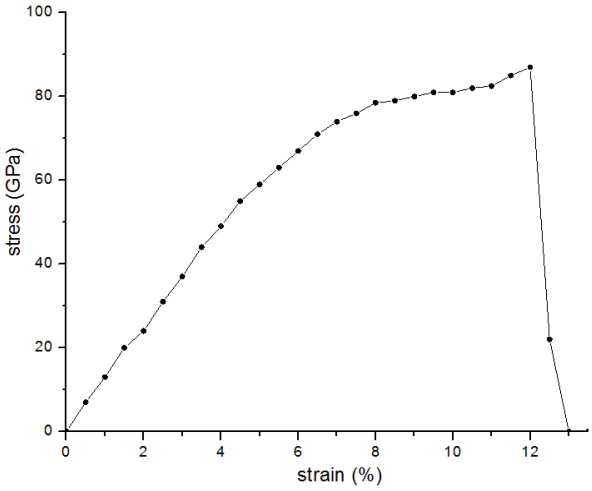

Fig. 1. Stress-strain characteristic calculated for an armchair (5, 5) SWCNT model of 2220 atoms.

At small strains, the tangent modulus is 1.19 TPa, close to other reported results of 1.16 TPa [6], and 1.07 TPa [8]. Considering secant modulus E_s defined in (3), for each value of strain we associate a value of E_s, with ε as the local strain and σ the corresponding stress value:

$$E_s = \left[\sigma(\varepsilon) - \sigma(\varepsilon_0)\right]/\varepsilon. \tag{3}$$

We find that for strains of 5% and 10%, the tangent modulus is 1.2 TPa and 0.81 TPa respectively, comparable with 0.85 TPa and 0.74 TPa obtained by Belytscko. Regarding the failure stress of the SWCNT, we got 86 GPa, compared to 93.5 GPa reported in [6].

It is important to mention that the radius modifications can increase the difference above than 4%, as estimated for armchair SWCNT [9]. The failure of the single wall carbon nanotube at elongations around 12% is comparable with various computational and experimental results [10–12].

4. Excitation of longitudinal elastic waves by a quick stretching of the bridged SWCNT at constant rate

The dynamic simulation is associated to the behaviour of a bridged SWCNT of 2220 atoms, after a longitudinal stretch with a time interval of 3 ps, at a rate of 0.1 Å/ps, 1.0 Å/ps, and 2.0 Å/ps, applied at the right extremity of the nanotube, with the left end fixed.

Figure 2a shows the results of a large session of computation configuring a detailed view of the strain redistribution along the carbon nanotubes revealed for 15 ps. The position along the tube is given on the horizontal axis counted in cell number, and the time in picoseconds is on the vertical axis. The cell unit is the assembly of atoms that generates the whole SWCNT by translation. The local variation of intra-cell distances related to tube deformation is represented by the degree of gray from white (at equilibrium) to black (when the distance between the tube cell is greater than the breaking condition considered at 2.2 Å). Compression does not occur in these cases because after the tube elongation for 3 ps, the extremities of SWCNT remain fixed.

An intense longitudinal deformation (LD) wave is generated when we apply a deformation at one end of the tube. This wave propagates along the SWCNT and is reflected at the both ends of the nanotube where the model assumes rigid coupling. The higher level of grey observed where the reflections take place indicate the increase of the local strain due to the amplitude growth by constructive interference between the incident and the reflected waves in front of the both anchored ends of the carbon nanotube.

The increase of the longitudinal deformation velocity from 0.1 Å/ps up to 2.0 Å/ps determines the change of the average strain from 0.1% up to 2.2%. The local deformation carried out by the LD wave is larger than the average value of strain, as indicated by the high level of gray in Figure 2a, at 2.0 Å/ps, presenting a clear picture of a nonlinear media. The high frequency pattern in the gray scale indicates the dominant waves propagating along the deformed SWCNT.

Figure 2b shows the details on the vibration spectra excited by nanotubes stretching at different rates in between 0.1 Å/ps and 2.0 Å/ps for a fixed time period of 3 ps. These spectra were calculated by applying Fourier transform to the time dependency of the longitudinal deformations associated to the 60^{th} unit-cell of the SWCNT. The data refers for the time period of 32 ps after the start of the nanotube deformation.

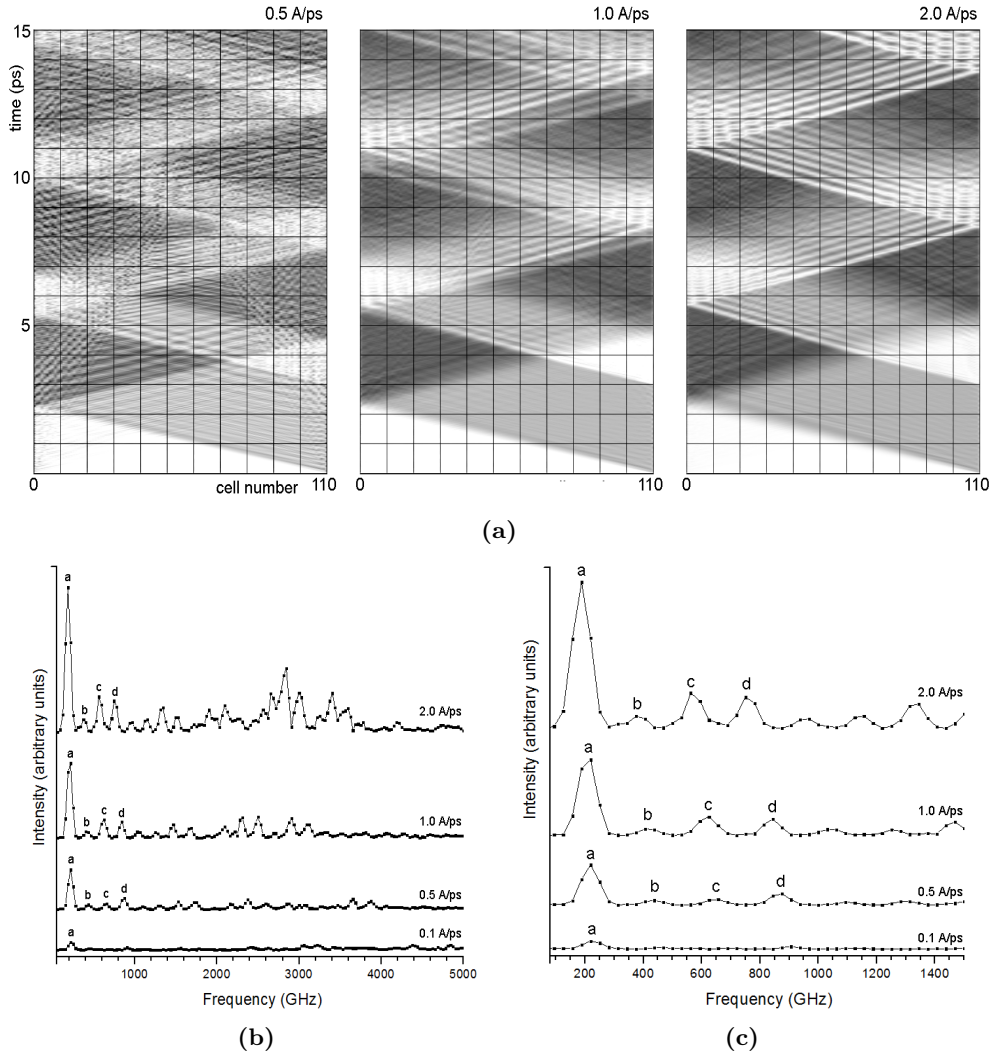

Fig. 2. a) The image of the elastic wave propagation along SWCNT produced by a quick stretching at a constant rate of 0.1 Å/ps, 1.0 Å/ps, and 3.0 Å/ps for 3 ps. The vertical scale shows the time passed from the initiation of the tube stretching applied at the right end of the tube, the other one being fixed at the origin of the axis. The horizontal axis represents the number of the elemental cell of (5,5) SWCNT counted from the left to the right. The level of gray indicates the local deformation of the tube calculated as the change of inter-unit cells distance relative to that representing the equilibrium state. The deformation is considered in modulus, so the compression and extension are represented by the same levels of dark gray. **b)** The frequency spectra excited by longitudinal deformation of SWCNT at different rates ranging from 0.1 Å/ps up to 3.0 Å/ps. **c)** This figure reveals more clearly the low frequency domain of the SWCNT response to its longitudinal deformation done at different velocities.

A part of the spectra is magnified in Fig. 2c, showing that the mechanical deformation conditions of a fixed time (3 ps) and different rates of stretching generates almost the same vibration frequencies in the stressed armchair (5, 5) SWCNT, considering the range of 0–1400 GHz. The peak marked as "a" around 200 GHz in Fig. 2b corresponds to the LD wave which gives the zigzag structure in Fig. 2a and the other as "b", "c" and "d" are represented by the interference like local patterns of the fine structure in the 2D picture.

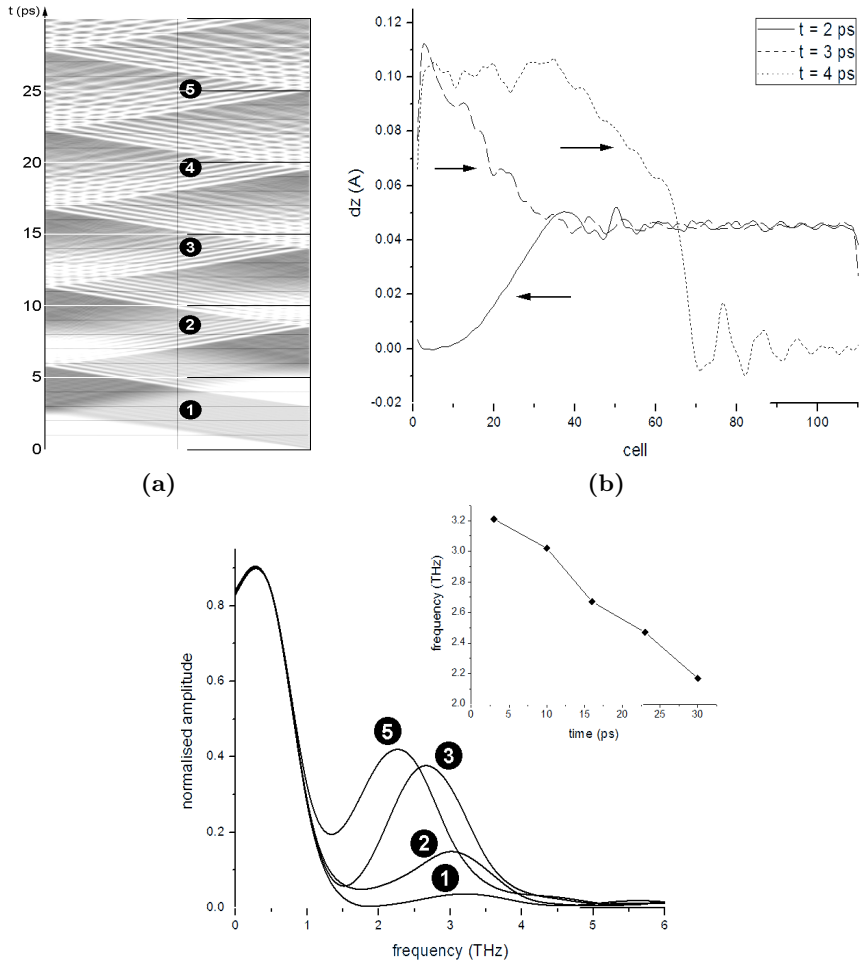

Fig. 3. a) Behaviour of the longitudinal waves in a deformed SWCNT tube, stretched for 3ps at a rate of 2 Å/ps. **b)** The frequency spectra is calculated by Fourier transform applied to the longitudinal oscillations collected near the middle of the tube when elastic waves passes through this position. **c)** Inter unit-cell distortion along the SWCNT corresponding to different stages of the LD wave propagation. Arrows indicate the incident and reflected LD wave near the left margin of the nanotube.

The whole picture of the elastic wave propagation in 32 picoseconds, being excited by the mechanical treatment of SWCNT stretching for 3 ps at a constant rate of 2.0 Å/ps, is given in Fig. 3a, to be related to the time behaviour of the vibrations frequencies. Each atom vibrates in its position with corresponding frequencies excited by the tube deformation. The spectra given in Fig. 3b results by using Fourier transform for collected position-time data of the longitudinal displacement of the cell unit placed close to the middle of SWCNT. Only those time intervals of 4 ps around the labels inserted in Fig. 2a were considered when LD wave is passing at the position of the 60th unit cell used to monitor the vibration frequencies. The resolution is lower than in Fig. 2 due to the small time intervals used, and the wide peaks are in fact envelopes of the vibrations showed in Fig. 2b for the two regions of the spectra centred at 0.2 THz and 3 THz respectively.

This analysis shows that the vibrations belonging to the band centered around 3 GHz has a continuous redshift in time after the nanotube deformation, as given in the inserted diagram. This result is correlated to the strain redistribution done by LD wave from the right to the left side of the tube, as it is seen in Fig. 3a, where the gray level becomes more and more uniformly distributed in time.

Figure 3c reveals better this process, indicating that inter-unit cell distances shown on the vertical axis increase continuously in time. The reflection of LD wave at the rigid ends of the SWCNT is also represented in this figure. As beyond these rigid limits no atoms are considered in the model to share the strain carried out by the incoming LD wave, the deformation of the tube is increased at both ends. A more realistic model must simulate the elastic coupling of the bridged SWCNT at its ends.

5. Excitation of longitudinal vibrations in bridged SWCNT by harmonic oscillation applied at one of the nanotube end

The second mechanical treatment of bridged SWCNT deformation was done by applying a forced harmonic oscillation along the nanotube axis at one end, the other being fixed. The longitudinal wave pattern given by reflections and interference is more complex. being generated by both compression and extension mechanical actions. Preliminary investigation on the oscillation modes induced in deformed carbon nanotubes was carried out by using a single cycle of the oscillator of 0.6 THz coupled at one end of the SWCNT.

A 2D picture of the generated elastic wave pattern is given in Fig. 4 for a nanotube initially in equilibrium, and for one under an initial strain of 9%, cooled by removing all of kinetic energy of the atoms. The generated elastic waves in the stressed tube have lower propagation velocity than in the relaxed one. The spread of the waves propagating from the right to the left in the time-space diagram is much larger in the case of the initially stressed nanotube. The ratio between the average velocities of the waves passing the nanotube in a relaxed state and that corresponding to strain of 9% is 2.3. This could be almost the highest value, considering that the strain of 9% is close to the disruption of the (5, 5) SWCNT as it is shown in Fig. 1.

The dispersion of the wave pattern after the second reflection in Figure 4a is an

indication of the capacity of disseminating the initial vibration energy received from the oscillator into the vibration modes of the carbon nanotube. This is not the case for the stressed SWCNT.

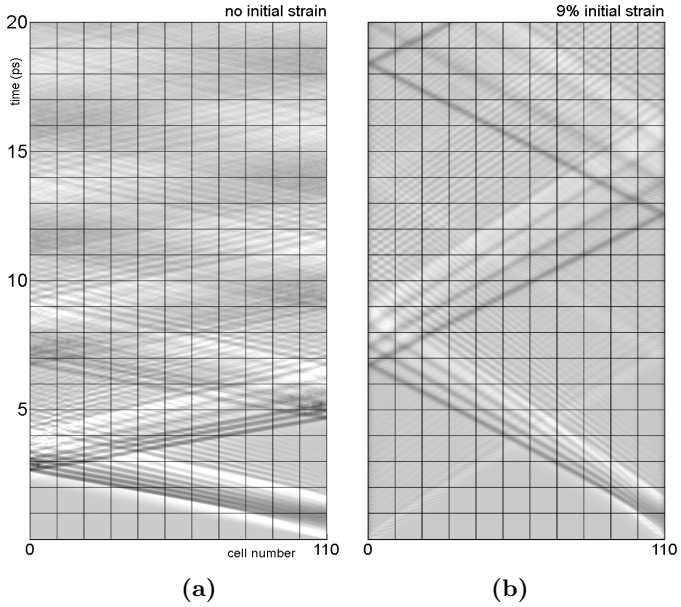

Fig. 4. SWCNT responses to its deformation by a harmonic forced oscillation acting at the right end of the nanotube for a single cycle. The coordinate system is the same as in Fig. 2a, the level of gray representing the local deformation, darker shade meaning compression and the local stretching between the nearest cells is indicated by low levels of gray up to white. **a)** Harmonic forced oscillation of 0.6 THz imposed to an unstressed, double clamped (5, 5) SWCNT at its right end. **b)** The same periodic deformation is applied against the same double clamped SWCNT , being initially stressed and equilibrated at a strain of 9%, which belongs to the non-linear region of stress-strain dependency (see Fig. 1).

6. Continuum deformation of the bridged SWCNT at constant rate

We extend this preliminary study to continuum stretching until the nanotube is broken. Figure 5a shows in the same way as in Fig. 2a the behaviour of longitudinal deformation waves along a carbon nanotube, initially unstressed, then stretched at a constant rate (2.63 Å/ps) at its right end until its failure. The very dark features at the upper side of the diagram correspond to the large distances between neighboring fragments relative to chemical bonds produced when SWCNT is broken.

After the initiation of the breaking site near the 9th unit-cell at 16.7 ps showed by the decreasing of the cross section of the SWCNT, other strong deformations take

place closed to the 27th unit-cell of the nanotube. An unexpected disruption of the nanotube takes place at this site, where the initiation of a fracture appears later than the one close to the 9th unit-cell (Fig. 5a). After this, a nanowire of carbon atoms is formed around the 9th unit-cell instead of fragment multiplication. The length of the carbon nanowire increases up to 21 Å after 17.4 ps counted from the start of the SWCNT stretching.

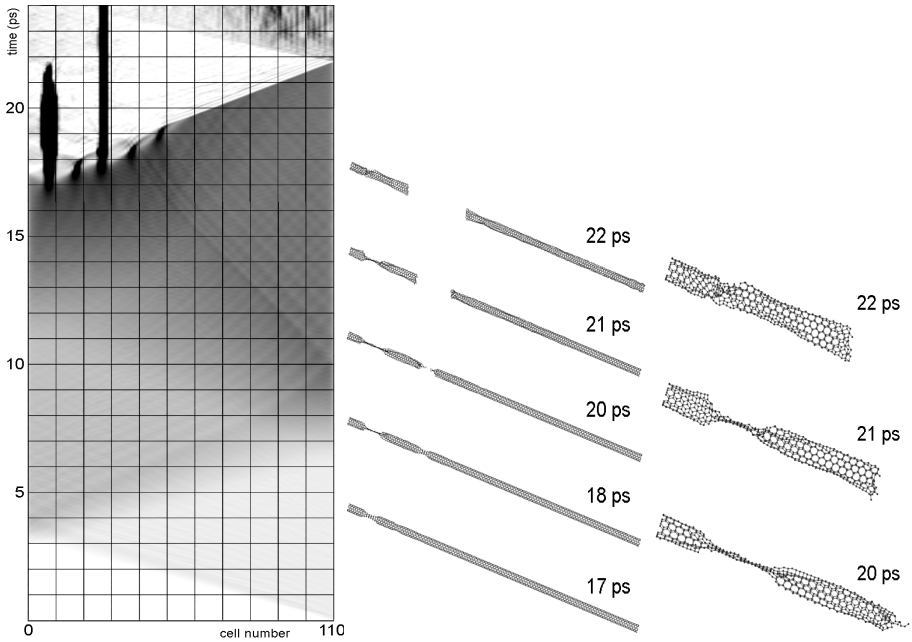

Fig. 5 a) The behaviour of the (5, 5) SWCNT deformed by continuous stretching at fixed rate of 2.63Å/ps until its final disruption into two segments (in 23 ps). The deep black regions at the top of the figure indicate the position where the nanotube breaks. The initiating fracture at the 9th unit-cell is reversible, the atoms preserve the chemical bonds by a phase transition to nanowire structure. The deformation close to the 28th unit-cell of (5, 5) SWCNT leads to an irreversible fracture of the nanotube. **b)** 3D images about the behaviour of the bridged SWCNT after 16 ps from the initiation of its stretching at a constant rate of 2.63 Å/ps. **c)** Zoom of the left margin of the (5, 5) SWCNT showing details of the transition to the carbon nanowire and the self healing of the defect.

The tube fails around the 27th unit-cell, making possible a fast compression in the resulting segments and facilitating the self-healing of the nano-tube structure at the site where the nanowire was formed. This happens after about 23 ps, as the diagrams of Fig. 5 indicate. At the end of the investigated period, the carbon nanotube failure leads to the formation of two SWCNTs having open ends. As the absolute variations of the intra-cell distance differences have been considered, the level of gray after tube fracture could also mean compression on Fig. 5a.

7. Conclusions

This study investigated the excited elastic waves in bridged SWCNTs produced by their deformation, considering three mechanical processes: short time deformation at constant rate, application of harmonic oscillations at one end of the nanotube, and continuum stretching until nanotube fracture. We investigate nonlinear behaviour on elastic wave propagation related to non-uniform distribution of strain along of carbon nanotube. The simulation based on molecular dynamics applied to a large atomistic model of 2200 atoms provides details about reversible / irreversible disruption of SWCNT, manifested by local transitions to carbon nanowire and self healing processes, as other authors already reported. The results presented above should be taken with care, as semi-quantitative ones, due to the approximation of the rigid coupling at both ends of the double clamped SWCNT. To improve the simulation it is needed to take into account the interaction between the carbon atoms at the tube margins and those of the substrates to which SWCNT is anchored.

References

[1] Selim M. M. *et al.*, *Effects of initial compression stress on wave propagation in carbon nanotubes*, Eur. Phys. J., B **69**, pp. 523–528, 2009.

[2] Rafii-Tabar H., *Computational modelling of thermo-mechanical and transport properties of carbon nanotubes*, Physics Reports, **390**, pp. 235–452, 2004.

[3] Rapaport D. C., *The Art of Molecular Dynamics Simulation*, Cambridge University Press, Cambridge, UK, 1995.

[4] Tersoff J., *New empirical approach for the structure and energy of covalent systems*, Phys. Rev., B **37**, pp. 6991–7000, 1988.

[5] Brenner D. W., *Empirical potential for hydrocarbons for use in simulating the chemical vapor deposition of diamond films*, Phys. Rev., B **42**, pp. 9458–9471, 1990.

[6] Belytschko T. *et al.*, *Atomistic simulations of nanotube fracture*, Phys. Rev., B **65**, pp. 235430–235437, 2002.

[7] Mylvaganam K., Zhang L. C., *Important issues in a molecular dynamics simulation for characterising the mechanical properties of carbon nanotubes*, Carbon, **42**, pp. 2025-2032, 2004.

[8] Yakobson B. I. *et al.*, *High strain rate fracture and C-chain unraveling in carbon nanotubes*, Comp. Mat. Sci., **8**, pp. 341–348, 1997.

[9] Agrawal P. M. *et al.*, *MD simulations of the dependence of C–C bond lengths and bond angles on the tensile strain in SWCNT*, Comp. Mat. Sci., **41**, pp. 450–456, 2008.

[10] Yu M. F. *et al.*, *Strength and Breaking Mechanism of Multiwalled Carbon Nanotubes Under Tensile Load*, Science, **287**, pp. 637–640, 2000.

[11] Yu M. F. *et al.*, *Tensile Loading of Ropes of SingleWall Carbon Nanotubes and their Mechanical Properties*, Phys. Rev. Lett., **84**, pp. 5552–5555, 2000.

[12] Buehler M. J., *Mesoscale modeling of mechanics of carbon nanotubes*, J. Mater. Res., **21**, pp. 2855–2869, 2006.